ACS BIO & MED CHEM Au
AN OPEN ACCESS JOURNAL OF THE AMERICAN CHEMICAL SOCIETY

pubs.acs.org/biomedchemau

Article

KRAS Inhibitor that Simultaneously Inhibits Nucleotide Exchange Activity and Effector Engagement

Cynthia V. Pagba, Amit K. Gupta, Ali K. Naji, Dharini van der Hoeven, Kelly Churion, Xiaowen Liang, Jacob Jakubec, Magnus Hook, Yan Zuo, Marisela Martinez de Kraatz, Jeffrey A. Frost, and Alemayehu A. Gorfe*

Cite This: *ACS Bio Med Chem Au* 2022, 2, 617–626

Read Online

ACCESS | Metrics & More | Article Recommendations | Supporting Information

ABSTRACT: We describe a small molecule ligand **ACA-14** (2-hydroxy-5-{[(2-phenylcyclopropyl) carbonyl] amino} benzoic acid) as an initial lead for the development of direct inhibitors of KRAS, a notoriously difficult anticancer drug target. We show that the compound binds to KRAS near the switch regions with affinities in the low micromolar range and exerts different effects on KRAS interactions with binding partners. Specifically, **ACA-14** impedes the interaction of KRAS with its effector Raf and reduces both intrinsic and SOS-mediated nucleotide exchange rates. Likely as a result of these effects, **ACA-14** inhibits signal transduction through the MAPK pathway in cells expressing mutant KRAS and inhibits the growth of pancreatic and colon cancer cells harboring mutant KRAS. We thus propose compound **ACA-14** as a useful initial lead for the development of broad-acting inhibitors that target multiple KRAS mutants and simultaneously deplete the fraction of GTP-loaded KRAS while abrogating the effector-binding ability of the already GTP-loaded fraction.

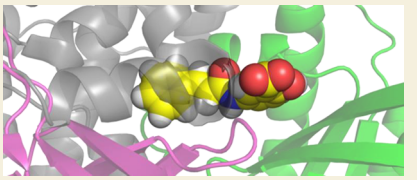

KEYWORDS: *Ras protein, inhibitor, signal transduction, anticancer drug, allosteric inhibition*

INTRODUCTION

RAS proteins are small GTPases that play crucial roles in cell signaling pathways that regulate cell growth and proliferation. They act as molecular switches by cycling between active GTP-bound and inactive GDP-bound conformational states. This cycle is regulated by GTPase activating proteins (GAPs) and nucleotide exchange factors (GEFs).[1] Mutations in RAS disrupt this process and result in constitutive activation, which then leads to uncontrolled cell growth, proliferation, and cancer.[2,3] Mutations in KRAS, one of the three most common human RAS proteins, are associated with ∼20% of all cancers, including >90% of pancreatic cancers, and >40% of colon cancers.[2,4,5] However, developing direct inhibitors of KRAS has been elusive[4,5] partly due to the very high affinity (picomolar)[6,7] of KRAS for its endogenous ligands GDP and GTP, which are abundant in the cell and prevent potential drugs from effectively competing for active site inhibition.[8−10] Hence, current efforts are directed toward allosteric inhibition. Our previous work,[11−14] along with that of others,[15−17] identified multiple allosteric sites/pockets that can potentially be targeted for inhibition by small molecules. Several small molecules that target these pockets and inhibit RAS activities have already been reported.[18−29] Covalent inhibitors targeting KRAS(G12C) are either in clinical trials (e.g., adagrasib) or recently approved by the FDA (sotorasib).[30−32] However, their application is limited to a few cancer types such as small cell lung cancer. Non-covalent allosteric inhibition will be needed to target many important KRAS mutations, including KRAS(G12D), KRAS(G12V), KRAS(G13D), and KRAS-(Q61H). These mutations account for >78% of KRAS-associated cancers[4,33] and are common in, among others, colon, lung, and pancreatic cancers. It is becoming increasingly clear that development of non-covalent KRAS inhibitors is possible, with the remaining challenges being overcoming problems of weak affinity and pan-RAS activity (e.g., refs 22, 34−36).

In the current work, we describe the KRAS binding and inhibitory profile of 2-hydroxy-5-{[(2-phenylcyclopropyl) carbonyl] amino} benzoic acid (**ACA-14**), which was predicted to target pocket p1 in our previous study combining molecular docking with nuclear magnetic resonance (NMR) experiments.[19] We found that **ACA-14** binds KRAS(WT) and various oncogenic KRAS mutants, including KRAS(G12D), in the low, single digit micromolar range but does not bind to HRAS or NRAS. The compound binds KRAS in a nucleotide state-independent manner and inhibits KRAS functions in biochemical assays by modulating both the intrinsic and GEF-mediated GDP/GTP exchange rates, as well as by directly disrupting effector binding. We also show that **ACA-14** inhibits MAPK signaling in KRAS(G12D)-expressing baby hamster

Received: July 8, 2022
Revised: August 27, 2022
Accepted: September 12, 2022
Published: September 26, 2022

https://doi.org/10.1021/acsbiomedchemau.2c00045
ACS Bio Med Chem Au 2022, 2, 617–626

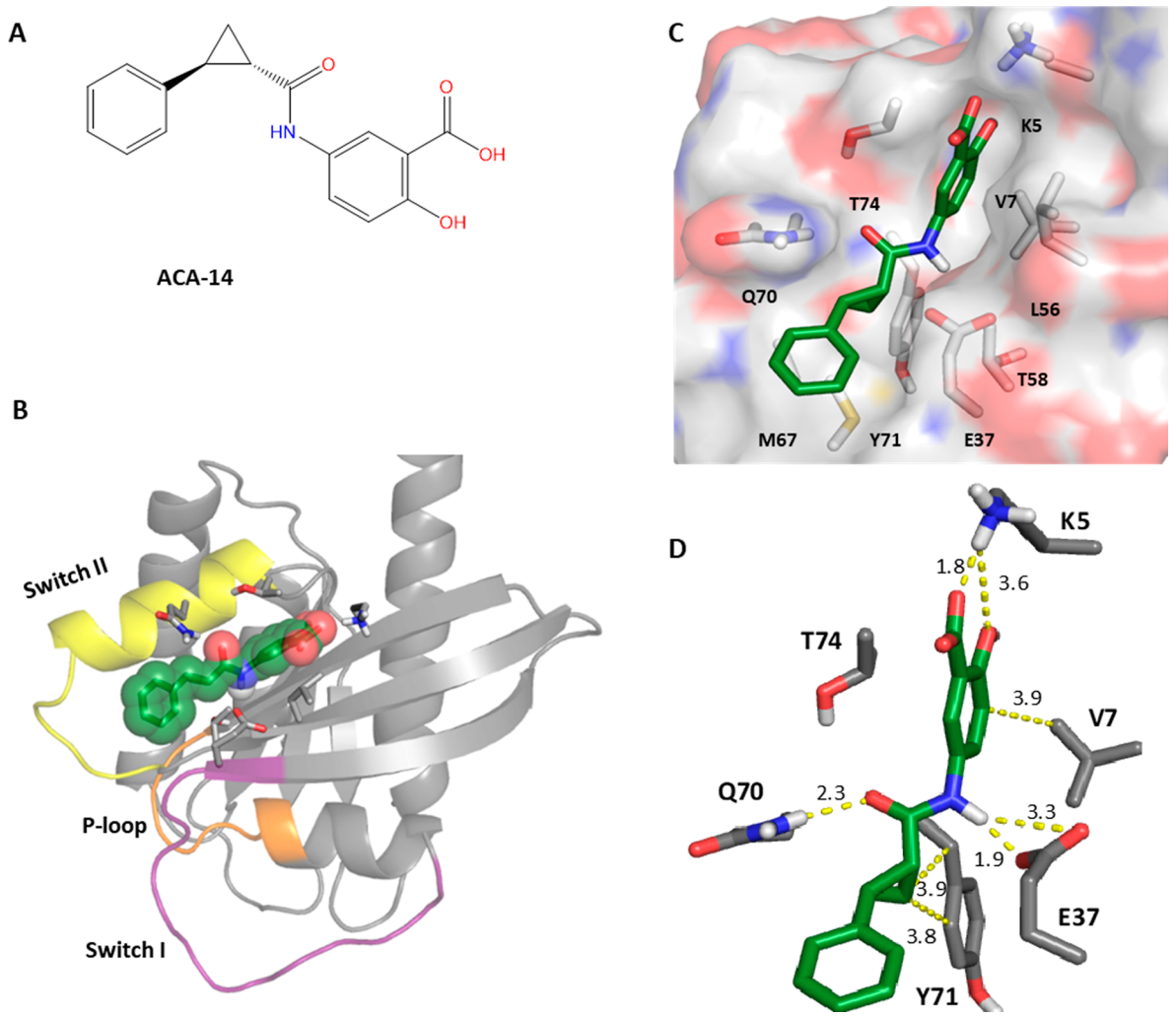

Figure 1. (A) Chemical structures of **ACA-14** (2-hydroxy-5-{[(2-phenylcyclopropyl) carbonyl] amino} benzoic acid). (B) Structure of GTP-KRAS(G12D)-derived from MD simulations, depicting pocket p1 occupied by **ACA-14** (green sticks and sphere). Structural regions near p1 involved in nucleotide binding and undergoing major conformational changes during GDP/GTP exchange are labeled: P-loop (orange, residues 10−17), switch I (purple, residues 25−40), and switch II (yellow, residues 60−74). Selected KRAS residues that are predicted to interact with the ligand are highlighted. (C,D) Detailed interactions of **ACA-14** (green sticks) with KRAS residues are shown in surface representation colored by electrostatic potential (C) or in a stick model (D).

kidney (BHK) cells, inhibits the proliferation of oncogenic KRAS-dependent cell lines, and reduces tumor growth in a KRAS(G12C)-driven MIAPaCa-2 xenograft mouse model. The cellular and *in vivo* activity profiles suggest a somewhat higher IC_{50} than suggested by the dissociation constants measured *in vitro* using truncated (residues 1−169) KRAS constructs, which we show is likely due to the limited cell permeability of the compound.

MATERIALS AND METHODS

Materials and detailed methods are provided in the Supporting Information. These include thermal shift assay (TSA), isothermal titration calorimetry (ITC), and fluorescence-based techniques such as microscale thermophoresis (MST) in purified systems for the determination of the binding affinity of **ACA-14** to wild type (WT) and some of the most prevalent oncogenic KRAS mutants including KRAS(G12D), KRAS(G12V), KRAS(G13D), KRAS(G12C), and KRAS(Q61H). Fluorescence-based techniques have also been used to biochemically characterize the inhibitory profile of the compound via the determination of the rates of intrinsic and SOS1 (a RAS GEF)-mediated nucleotide exchange and release reactions in KRAS(WT), and the interactions of KRAS(WT) with the RAS binding domain (RBD) of c-Raf. Additional experiments include cell-based pull-down and immunoblotting assays to examine the ability of **ACA-14** to inhibit KRAS(G12D)−RafRBD interactions and KRAS(G12D)-mediated signaling through the MAPK pathway, as well as cell proliferation assays to examine the impact of the ligand on the growth of a variety of cancer cell lineages. The compound has also been tested in an *in vivo* setting using a xenograft mouse tumor model, as detailed in the Supporting Information.

RESULTS AND DISCUSSION

Figure 1A displays the chemical structure of compound **ACA-14** (cLogP = 3.35) that we have previously identified as a KRAS binder based on combined computational and NMR analyses (named compound V14 in ref 19). However, the previous work did not go beyond the detection of **ACA-14** binding to KRAS. We have now conducted an extensive structure/activity relationship analysis and summarize our findings as follows.

https://doi.org/10.1021/acsbiomedchemau.2c00045
ACS Bio Med Chem Au 2022, 2, 617−626

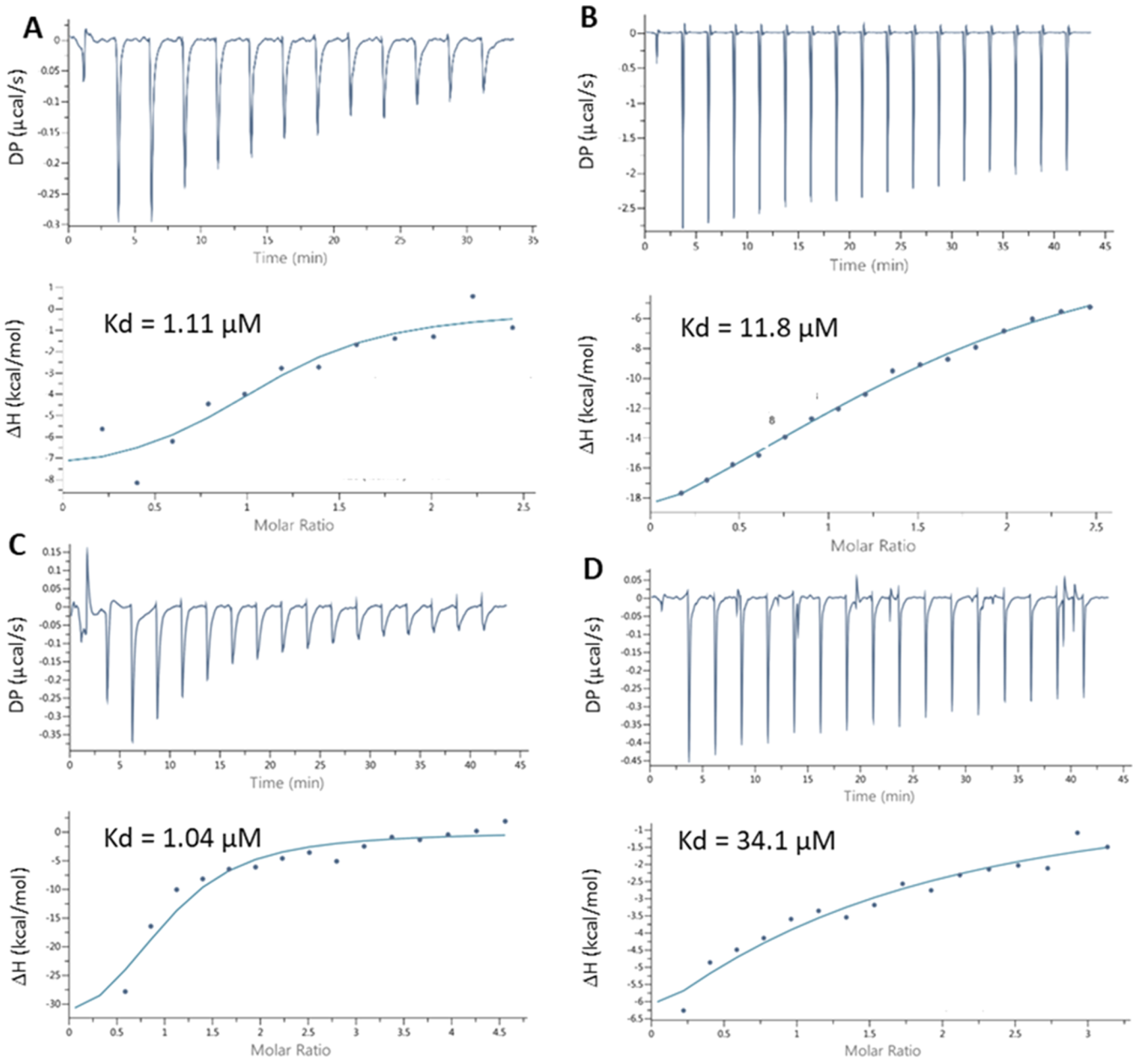

Figure 2. ITC profiles of **ACA-14** with (A) GDP-KRAS(WT), (B) GDP-KRAS(G12C), (C) GDP-KRAS(Q61H), and (D) GDP-KRAS(G13D) obtained using Malvern's MicroCal PEAQ-ITC.

Predicted Binding Pose of ACA-14 at the p1 Pocket of KRAS

A common target for **ACA-14** and another series of previously reported compounds[21] was pocket p1. The predicted binding pose of **ACA-14** and KRAS residues involved in interactions with the ligand are shown in Figure 1B–D. Among these are a carboxyl oxygen from the benzoic acid moiety of **ACA-14** being within a H-bonding distance (1.8 Å) from the amino group of K5, and the NH substituent that is 1.9 Å away from the side-chain carboxyl oxygen of E37 at the effector-binding loop. The phenyl ring of the ligand is 3.9 Å away from the side chains of V7 and L56, suggesting van der Waals (vdW) contacts between them. Moreover, the carbonyl group near the phenylcyclopropyl moiety is within a H-bonding distance (2.3 Å) from Q70 while the cyclopropyl ring is within a vdW distance from Y71. These residues are part of switch 2, which is crucial in structural rearrangements that accompany nucleotide exchange.

ACA-14 Binds to Active and Inactive WT and Oncogenic KRAS Mutants with Low Micromolar Affinity

We used two orthogonal assays in purified systems to assess whether **ACA-14** directly interacts with KRAS: TSA and intrinsic fluorescence (IF). TSA is commonly used to monitor protein–ligand complex formation based on the principle that ligand binding alters the thermal stability [i.e., the melting temperature (T_m)] of the protein.[37,38] The TSA profiles, as shown in Figure S1, indicate shifts in the Tm of GNP (GTP-analogue)-bound WT and selected KRAS mutants in the presence of 50 μM **ACA-14**, suggesting structural changes induced by ligand binding (Figure S1A–C). Interestingly, there is no measurable change in the Tm of NRAS and HRAS, which are close homologues of KRAS, when mixed with the

https://doi.org/10.1021/acsbiomedchemau.2c00045
ACS Bio Med Chem Au 2022, 2, 617–626

same concentration of the compound (Figure S1D,E). This shows that **ACA-14** interacts with KRAS in an isoform-specific manner. We also detected direct binding of **ACA-14** to KRAS by taking advantage of the weak IF of the compound. Figure S2 displays concentration-dependent changes in the IF of the compound upon mixing varying concentrations of **ACA-14** with fixed concentrations of KRAS(WT) or KRAS(G12D). While the weak fluorescence precludes quantitative detection of K_ds using IF, the TSA and IF results together establish the direct binding of **ACA-14** to both GTP- and GDP-bound KRAS(WT), KRAS(G12D), and KRAS(Q61H) but not to HRAS(WT) and NRAS(WT).

We used MST and ITC for a more quantitative assessment of the ligand−KRAS interactions. Representative titration/binding curves from both ITC and MST are shown in Figures 2 and S3, respectively, and Table 1 summarizes equilibrium

Table 1. Summary of Equilibrium Dissociation Constant (K_d) Values Derived from MST and ITC[a]

	K_d (μM) from MST or (ITC)	
KRAS	GDP-bound	GNP-bound
WT	4.5 ± 1.5 (1.1 ± 1.6)	0.05 ± 0.03; 10.0 ± 1.7[b]
G12D	>50 (45.9)	0.35 ± 0.08; 2.5 ± 0.4[b]
G12C	(11.8 ± 5.49)	0.34 ± 0.07
Q61H	(1.04 ± 0.63)	0.02 ± 0.01; 3.5 ± 1.5[b]
G12V	ND	ND
G13D	(34.1)	ND

[a]ND = not determined (data were noisy). [b]The two K_ds suggest the possibility of two binding sites with different affinities.

dissociation constants derived from those curves. One can see that, first, MST and ITC yielded comparable K_d values for GDP-bound KRAS(WT) and KRAS(G12D), which provides confidence in the reliability of the MST data. Second, the combined MST and ITC results make clear that **ACA-14** binds to both GDP-bound and GNP-bound forms of WT and most KRAS mutants, with the exception of GDP/GNP-KRAS-(G12V) and GNP-KRAS(G13D), for which the MST data were noisy. An enthalpy-dominated (Figure 2) binding with K_d ≈ 1.0−50 μM (Table 1) was measured for the GDP-KRAS proteins. An enthalpy-dominated interaction of **ACA-14** and KRAS is consistent with the substantial number of predicted hydrogen bonding and vdW interactions (Figure 1). The MST binding curves for GNP-bound KRAS(WT), KRAS(G12D), and KRAS(Q61H) suggest two transition events (Figure S3B,C) and dissociation constants (Table 1): a high affinity binding event with K_d ≈ 50−400 nM and a lower affinity binding event with K_d ≈ 3−10 μM. Preliminary ITC measurements also suggest the existence of an entropy-dominated, high-affinity binding event in GNP-bound KRAS, but the data were too noisy for quantitative analysis (not shown). A two-step transition in MST binding curves may suggest ligand binding at two different sites, which is possible because KRAS harbors multiple ligand-binding sites. For example, **ACA-14** may bind KRAS at pockets p1 and p2 with different affinities. Alternatively, different isomers of **ACA-14** may bind at the same pocket with different affinities. Resolving these issues by solving co-crystal structures, for example, would allow for a more complete structure−activity relationship study focused on identifying features that favor selective binding to activated KRAS. The current work, however, focuses on the weaker binding mode that is shared by the active and inactive forms of KRAS because it is more consistent with data from functional assays discussed in subsequent sections. Binding in the low micromolar range is also consistent with the docking results, which predicted binding free energies in the range of −6.5 to −7.5 kcal/mol at pocket p1.

The combined data from TSA, IF, MST, and ITC demonstrate that **ACA-14** is likely a pan-KRAS binder and interacts with both the active and inactive forms of WT and most of the prevalent oncogenic KRAS mutants with a single-to-double digit micromolar binding affinity. Still, there is up to five-fold difference in K_d among the various mutants in the GDP state [e.g., compare KRAS(Q61H) and KRAS(G12D) in Table 1] and up to a 10-fold difference among those in the GTP state (G12C vs WT; Table 1). This may be explained by the significant differences among KRAS mutants in dynamics, particularly at the flexible switch regions that undergo conformational changes during nucleotide exchange and GTP hydrolysis,[39−43] or by variations in the physicochemical properties of pocket p1 among oncogenic KRAS mutants.[19] Similarly, GDP-bound and GNP-bound KRAS differ at switch 1 and switch 2.[40,44−46] Such structural changes may result in the rearrangement of residues proximal to ligand-binding sites p1 or p2.

ACA-14 Modulates Nucleotide Exchange and Disrupts Effector Binding

To examine the potential effects of **ACA-14** on KRAS functions, we used fluorescent-based biochemical assays to monitor the rates of nucleotide dissociation or exchange reactions of KRAS, as well as interaction of KRAS with the RBD of its effector c-Raf. We found that **ACA-14** modulates nucleotide exchange (Figure 3) but not GDP release/dissociation (Figure S4). Specifically, **ACA-14** reduced the rates of both intrinsic and SOS-mediated GDP/GTP exchange reactions in a dose-dependent manner, with EC_{50} of 3.8 ± 0.6 and 2.1 ± 0.4 μM, respectively (Figure 3A,B). These EC_{50} values are remarkably close to the K_d of **ACA-14** for KRAS(WT), as assessed by MST and ITC (Table 1), providing additional evidence for direct binding. The lack of effect on the rate of intrinsic or SOS-mediated GDP release (Figure S4) suggests that, while able to bind to the GDP state, **ACA-14** may not directly affect the conformation of residues involved in GDP dissociation and/or SOS binding (see, e.g., refs 27 47, and 48 for how SOS interacts with GDP-RAS). Its effect on GDP/GTP exchange may therefore be associated with **ACA-14** sterically or allosterically hindering GTP loading, altering the structure of the nucleotide-free KRAS/SOS complex,[49] or interfering with SOS binding to activated KRAS(WT) by altering the orientation of residues in the switch 2 region.[27,47]

To evaluate the effect of **ACA-14** on effector binding, we measured the affinity of BODIPY-GTP-γ-S (BGTP)-bound KRAS(WT) to RBD using fluorescence polarization (FP) assay (Figure 4A). The dissociation constant for the interaction of BGTP-KRAS and RBD (K_d = 1.15 ± 0.09 μM) increased by a factor of ∼5 (K_d = 6.14 ± 1.86 μM) in the presence of 20 μM **ACA-14**. This result is consistent with data from pull-down assay using BHK cells expressing GFP-tagged KRAS(G12D) (Figure 4B−D). The level of GFP-tagged GTP-KRAS(G12D) and endogenous RAS pulled down by the c-Raf RBD was significantly reduced when lysates were treated with 10 μM or more of the ligand. These results strongly suggest that **ACA-14** inhibits the binding of KRAS to its effector c-Raf,

https://doi.org/10.1021/acsbiomedchemau.2c00045
ACS Bio Med Chem Au 2022, 2, 617−626

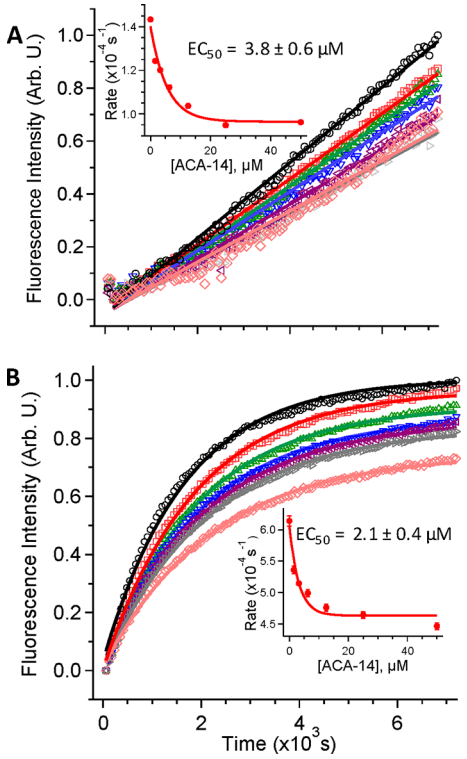

Figure 3. Effect of **ACA-14** on the intrinsic (A) and SOS-mediated (B) nucleotide exchange rates determined by monitoring the change in fluorescence intensity increase in BGTP upon binding to KRAS. Ligand concentrations: 0 (black circle), 1.56 (red square), 3.12 (green triangle), 6.25 (blue inverted triangle), 12 (purple left-sided triangle), 25 (gray right-sided triangle), and 50 μM (light-orange diamond). Fluorescence intensity (I) was normalized using the formula:[27] $I_{normalized} = (I_{raw} - I_0)/(I_{max} - I_0)$ where I_{raw} is the fluorescence intensity at a given time, I_0 is the intensity at 60 s, and I_{max} is the maximum fluorescence (of KRAS alone) at the end of the experiment. Linear (A) or single exponential (B) fits are superimposed as solid lines. Inset: calculated rates ($\times 10^{-4}$ s^{-1}) as a function of ligand concentrations; EC_{50} values derived by fitting the curves are shown. KRAS, BGTP, and SOS concentrations were 0.5 μM each, and the buffer (pH 7.5) contained 25 mM Tris Cl, 50 mM NaCl, and 10 mM $MgCl_2$.

possibly by blocking KRAS residues involved in c-Raf binding (such as the effector-interacting E37,[50] see Figure 1D). Together, our analyses using purified proteins and cell lysates demonstrate that **ACA-14** modulates KRAS functions by both decelerating the rate of nucleotide exchange and impeding interaction with effector proteins. The ability of **ACA-14** to bind both the active and inactive forms of KRAS likely explains its dual action. We propose that such broad-acting KRAS inhibitors can have major therapeutic value upon further optimization because they have the potential to simultaneously deplete the fraction of GTP-loaded KRAS while abrogating the effector-binding ability of the already GTP-loaded fraction.

ACA-14 Inhibits Signaling through the MAPK Pathway and the Proliferation of Cancer Cells Expressing Mutant KRAS

We used cell signaling and proliferation assays to check whether the inhibitory activities of **ACA-14** observed in the biophysical and pulldown assays described above translated into inhibitory activities in the cell. In the signaling assays, BHK cells expressing KRAS(G12D) were treated with compound or DMSO control, and the levels of phosphorylated KRAS effectors were monitored by immunoblotting. Figure 4E–H shows that **ACA-14** significantly reduced the levels of phosphorylated c-Raf (p-cRaf) and ERK (p-ERK) but had little effect on p-AKT levels in the concentration range tested. This suggests that **ACA-14** selectively inhibits KRAS signaling through the MAPK pathway, consistent with its effect on the interaction of KRAS(WT) with RafRBD (Figure 4A–D).

We then examined the inhibitory effects of **ACA-14** on cell proliferation using selected colon and pancreatic cancer cell lines (Figure 5A). Up to 100 μM of **ACA-14** had no effect on the proliferation of the KRAS-independent BxPC-3 [pancreatic adenocarcinoma cells expressing KRAS(WT)], CaCO-2 [a colon cancer cell harboring KRAS(WT)], or HPNE [normal, immortalized pancreatic duct cells with KRAS(WT)]. On the other hand, treatment with 25–100 μM of **ACA-14** significantly inhibited the proliferation of pancreatic cancer cells that express mutant KRAS, including KRAS(G12C) (MIAPaCa-2), KRAS(G12R) (MOH), and KRAS(G12D) (PANC-1). These are all KRAS-dependent cell lines (see, e.g., ref 51 and references therein). We obtained similar results for the colon cancer cell lines SW116 and SW948 (Figure 5A), which harbor KRAS(G12A) and KRAS(Q61L), respectively.[52] The higher concentration (>20 μM) required to inhibit MAPK signaling (Figure 4) or the proliferation of cancer cells expressing various mutants of KRAS (Figure 5A) may be due to the weak cell permeability of the ligand. This is supported by data from initial permeability tests in a MDR1-MDCK cell monolayer system (Table 2), which show that the rate of permeability of **ACA-14** into the cell is about six-fold less than that for the control ligand propranolol, which has high cell permeability. Table 2 also shows that the efflux ratio of **ACA-14** (0.72 nm/s) is comparable to that of propranolol (0.52 nm/s) but differs from amprenavir by 24-fold. Amprenavir is a known substrate of the efflux pump P-glycoprotein (Pg-P) while propranolol is not (note: efflux ratio >2.0 indicates that a ligand is a Pg-P substrate). This result suggests that once in the cell, **ACA-14** is not readily expelled and thus likely has a long half-life and good bioavailability. Indeed, we found that **ACA-14** exhibits a very low rate of intrinsic clearance (<0.3 mL/min/g) and has a long half-life in mouse, rat, and human microsomes (>180 min). Interestingly, this activity profile mirrors that of the previously reported KRAS(G12D) inhibitor, BI-2852 (Kessler, et al.[20]), which binds with high affinity (~700 nM) and inhibits SOS and Raf with 500–700 nM IC_{50} *in vitro* but exhibits low μM IC_{50} against cancer cell lines harboring mutant KRAS.

ACA-14 Inhibits Tumor Growth

To assess the anti-tumor efficacy of **ACA-14**, we tested its ability to inhibit MIAPaCa-2 xenograft tumor growth. MIAPaCa-2 cells harbor homozygous KRAS(G12C) mutations and require oncogenic KRAS for tumor growth.[53,54] Nude mice were injected subcutaneously in the hind flank with MIAPaCa-2 cells. After 3 days, tumor volumes were measured, and the mice were separated into two treatment groups with equal mean tumor volumes. Mice were then treated 5 days per week with intraperitoneal injections of either **ACA-14** (5 mg/kg) or vehicle (corn oil). Tumor volumes were measured twice per week with electronic calipers. Mice weights were measured once per week. When control tumors reached an average of 2 cm^3, all mice were euthanized. We observed that **ACA-14** treatment caused a small but statistically significant reduction in tumor growth that was maintained until day 20 (Figure

https://doi.org/10.1021/acsbiomedchemau.2c00045
ACS Bio Med Chem Au 2022, 2, 617–626

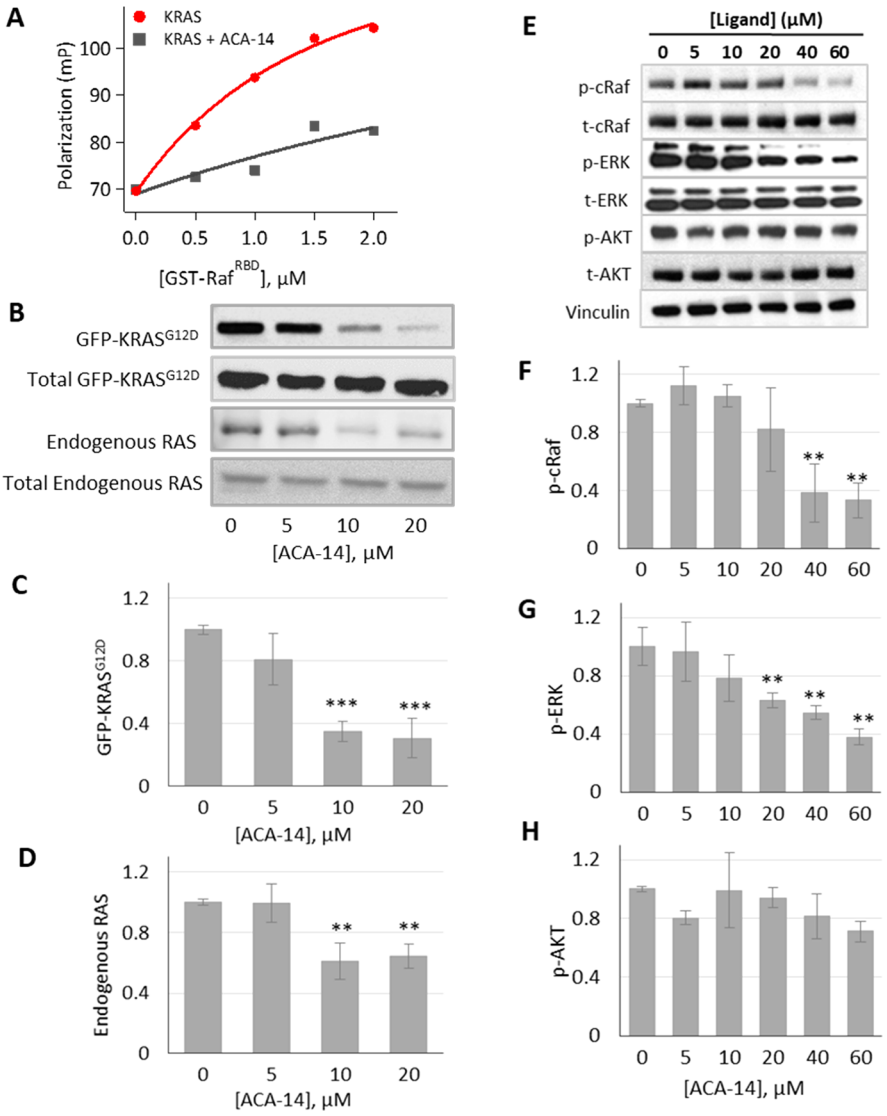

Figure 4. ACA-14 disrupts KRAS-Raf interaction (A–D) and inhibits MAPK signaling (E–H). (A) Effect of **ACA-14** on the interaction of varying concentrations of GST-RBD of Raf with 0.5 μM BGTP-γ-S-KRAS in the absence (red; K_d = 6.14 ± 1.86 μM) and presence of 20 μM **ACA-14** (1.15 ± 0.09). The dissociation constant (K_d) was derived from the quadratic ligand-binding equation[55,56] $P = P1 + (P2 - P1)\frac{K_d + c + x - \sqrt{(K_d + c + x)^2 - 4 \times c \times x}}{2}$, where P1 and P2 are polarization of free and RBD-bound KRAS, respectively, c is the total concentration of KRAS, and x is the total concentration of RBD. (B–D) Representative western blots, including loading controls total GFP-KRAS(G12D) and total endogenous RAS (B), level of GFP-tagged GTP-KRAS(G12D) (C), and endogenous RAS (D) pulled-down by GST-RBD after treatment of BHK cell lysates ectopically expressing GFP-tagged KRAS(G12D) with increasing concentrations of **ACA-14**. (E) Representative western blots of whole cell lysates from BHK cells expressing GFP-tagged KRAS(G12D) treated for 3 h with vehicle (DMSO) or the indicated concentrations of **ACA-14** under serum-starved condition. Vinculin was used as a loading control. (F–H) Quantitation of the levels of phosphorylated c-Raf (p-cRaf) (F), ERK (p-ERK) (G), and AKT (p-AKT) (H). (C,D,F–H) Values are normalized against DMSO control and averaged from three independent experiments. Statistical significance was calculated between vehicle (DMSO) and compound-treated samples using unpaired Student's t test.

5B,C). After that time, a trend toward reduced tumor growth was maintained, but statistical significance was lost due to variability in tumor sizes. Importantly, **ACA-14** appeared to be well tolerated as it did not affect weight gain in treated mice (Figure 5D). We also measured ERK activation in tumor lysates as readout for KRAS inhibition. We observed that **ACA-14** treatment caused a small but significant reduction in ERK activation within tumors (Figure 5E,F). These data indicate that **ACA-14** is well tolerated in mice and is capable of inhibiting tumor growth *in vivo*.

CONCLUSIONS

In this work, we describe the small molecule **ACA-14** as a lead compound for the development of therapies that directly act on KRAS to inhibit its abnormal signaling activities. We have shown that the compound binds to KRAS in a nucleotide-independent manner with affinities in the single-digit micromolar range, likely targeting a pocket formed by residues from the three N-terminal beta-strands and the switch regions of KRAS, or between helices 2 and 3. These sites have been previously characterized as robust targets for small-molecule binding. Using a variety of biophysical and cell biological

https://doi.org/10.1021/acsbiomedchemau.2c00045
ACS Bio Med Chem Au 2022, 2, 617–626

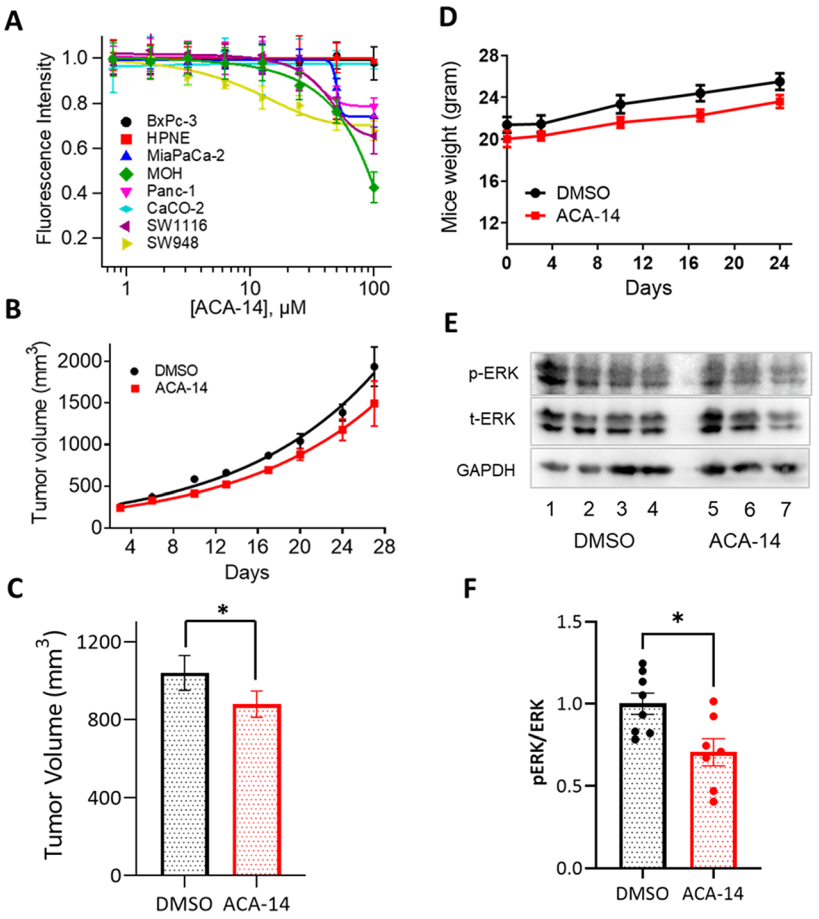

Figure 5. Effect of **ACA-14** on the proliferation of pancreatic cells and tumor growth. (A) Effect of **ACA-14** on the proliferation of pancreatic (BxPC-3, HPNE, MIAPaCa-2, MOH, and Panc-1) and colon (CaCO-2, SW948, and SW1116) cancer cell lines. (B) Effect of **ACA-14** on MIAPaCa-2 subcutaneous tumor growth. **ACA-14** was administered intraperitoneally at 5 mg/kg, diluted in corn oil. Controls are an equal volume of diluent (DMSO) added to corn oil alone. Tumor sizes were measured using electronic calipers, and tumor volumes were calculated using the formula volume = (length × width^2)/2. Shown are the average tumor volumes for control (n = 8) and **ACA-14**-treated mice (n = 7). Errors are standard error of the mean (SEM). (C) Volume of tumor on day 20 of the experiment. (D) Weights of DMSO and **ACA-14**-treated mice. Mice were weighed once per week. Errors are SEM. (E) Representative western blots for p-ERK, total ERK, and GAPDH in DMSO (lanes 1 to 4) and **ACA-14** (lanes 5 to 7)-treated tumors. (F) Quantification of p-ERK western blots in DMSO (n = 8) and **ACA-14** (n = 7)-treated tumors. Errors are SEM * = p<0.05.

Table 2. Permeability and Efflux of ACA-14 in a MDR1-MDCK Cell Monolayer System[a]

	ACA-14	amprenavir	propranolol
$P_{apparent}$, A > B (nm/s)	54.25	16.52	312.08
$P_{apparent}$, B > A (nm/s)	35.14	170.98	150.01
$P_{apparent}$ efflux ratio (ER)	0.65	10.35	0.48
P_{exact}, A > B (nm/s)	53.55	14.36	399.79
P_{exact}, B > A (nm/s)	38.33	243.25	207.15
P_{exact} efflux ratio	0.72	16.93	0.52

[a]This experiment was conducted by *Alliance Pharma* as paid service. Propranolol and amprenavir are used, respectively, as a non P-gp-dependent high transcellular permeability marker and a positive control for P-gp efflux activity. $P_{apparent}$ is the membrane permeability index of the compound (donor) determined by considering only two-compartment system (donor and receiver). P_{exact} corrects for the volume occupied by the cells in the donor side of the membrane.

assays, including FP, signaling, and pull-down assays, we have shown that **ACA-14** impedes the interaction of KRAS with the RBD of its effector c-Raf and reduces the rates of intrinsic and GEF-mediated exchange of GDP to GTP. As a result, the ligand inhibits signal transduction through the MAPK pathway in cells expressing mutant KRAS, as assessed by monitoring the levels of phosphorylated c-Raf and ERK. It also inhibits the growth of pancreatic and colon cancer cells harboring mutant but not WT KRAS and attenuates tumor growth in a xenograft mouse tumor model. Compared to its effects in biochemical assays outside the cell, the inhibitory activities of **ACA-14** in the cell required the use of slightly higher concentrations. One reason for this could be a smaller effective concentration in the cell due to limited cell permeability. This is supported by results from permeability assays, which suggest that, while the ligand is not a Pg-P substrate, there is room for improvement regarding its cell permeability. Since it is amenable to a range of chemical modifications to address these issues, we propose **ACA-14** as a starting point for developing leads toward dual-acting KRAS inhibitors that target a wide variety of cancers driven by G12, G13, and Q61 KRAS mutations.

https://doi.org/10.1021/acsbiomedchemau.2c00045
ACS Bio Med Chem Au 2022, 2, 617−626

■ ASSOCIATED CONTENT

Supporting Information

The Supporting Information is available free of charge at https://pubs.acs.org/doi/10.1021/acsbiomedchemau.2c00045.

Detailed methodologies, TSA, IF of **ACA-14** with and without KRAS, MST assay, and effect of **ACA-14** ligand on the intrinsic and SOS-mediated nucleotide release rates (PDF)

■ AUTHOR INFORMATION

Corresponding Author

Alemayehu A. Gorfe − *Department of Integrative Biology and Pharmacology, McGovern Medical School, The University of Texas Health Science Center at Houston, Houston, Texas 77030, United States; Biochemistry and Cell Biology Program & Therapeutics and Pharmacology Program, UTHealth MD Anderson Cancer Center Graduate School of Biomedical Sciences, Houston, Texas 77030, United States;* orcid.org/0000-0002-9328-4692; Email: alemayehu.g.abebe@uth.tmc.edu

Authors

Cynthia V. Pagba − *Department of Integrative Biology and Pharmacology, McGovern Medical School, The University of Texas Health Science Center at Houston, Houston, Texas 77030, United States;* orcid.org/0000-0002-3642-4361

Amit K. Gupta − *Department of Integrative Biology and Pharmacology, McGovern Medical School, The University of Texas Health Science Center at Houston, Houston, Texas 77030, United States*

Ali K. Naji − *Department of Diagnostic and Biomedical Sciences, School of Dentistry, The University of Texas Health Science Center at Houston, Houston, Texas 77030, United States*

Dharini van der Hoeven − *Department of Diagnostic and Biomedical Sciences, School of Dentistry, The University of Texas Health Science Center at Houston, Houston, Texas 77030, United States*

Kelly Churion − *Center for Infectious and Inflammatory Diseases, Texas A&M University Health Science Center, Houston, Texas 77030, United States*

Xiaowen Liang − *Department of Integrative Biology and Pharmacology, McGovern Medical School, The University of Texas Health Science Center at Houston, Houston, Texas 77030, United States;* orcid.org/0000-0002-6174-2951

Jacob Jakubec − *Department of Integrative Biology and Pharmacology, McGovern Medical School, The University of Texas Health Science Center at Houston, Houston, Texas 77030, United States*

Magnus Hook − *Center for Infectious and Inflammatory Diseases, Texas A&M University Health Science Center, Houston, Texas 77030, United States*

Yan Zuo − *Department of Integrative Biology and Pharmacology, McGovern Medical School, The University of Texas Health Science Center at Houston, Houston, Texas 77030, United States*

Marisela Martinez de Kraatz − *Department of Integrative Biology and Pharmacology, McGovern Medical School, The University of Texas Health Science Center at Houston, Houston, Texas 77030, United States*

Jeffrey A. Frost − *Department of Integrative Biology and Pharmacology, McGovern Medical School, The University of Texas Health Science Center at Houston, Houston, Texas 77030, United States; Biochemistry and Cell Biology Program, UTHealth MD Anderson Cancer Center Graduate School of Biomedical Sciences, Houston, Texas 77030, United States*

Complete contact information is available at: https://pubs.acs.org/10.1021/acsbiomedchemau.2c00045

Author Contributions

CRediT: **Cynthia V Pagba** conceptualization (supporting), data curation (lead), formal analysis (equal), methodology (lead), software (lead), writing-original draft (equal), writing-review & editing (equal); **Amit K Gupta** conceptualization (supporting), data curation (supporting), formal analysis (supporting), methodology (supporting), software (supporting), writing-original draft (supporting), writing-review & editing (supporting); **Ali K Naji** methodology (supporting), software (supporting); **Dharini van der Hoeven** methodology (supporting), software (supporting); **Kelly Churion** methodology (supporting), software (supporting); **Xiaowen Liang** methodology (supporting), software (supporting), writing-original draft (supporting); **Jacob Jakubec** methodology (supporting); **Magnus Hook** formal analysis (supporting), methodology (supporting); **Yan Zuo** methodology (supporting), software (supporting), writing-original draft (supporting), writing-review & editing (supporting); **Marisela Martinez de Kraatz** methodology (supporting); **Jeffrey A Frost** formal analysis (supporting), methodology (supporting), writing-original draft (supporting), writing-review & editing (supporting); **Alemayehu A. Gorfe** conceptualization (lead), formal analysis (equal), funding acquisition (lead), investigation (lead), methodology (lead), project administration (lead), resources (lead), supervision (lead), writing-original draft (lead), writing-review & editing (equal).

Notes

The authors declare no competing financial interest.

■ ACKNOWLEDGMENTS

We are grateful to Drs. John Hancock and Yong Zhou (UTHealth) for illuminating discussions, Xiaodong Cheng (UTHealth) for making his NanoTemper MST instrument freely available to us, and Carla Mattos (Northeastern University) and John Putkey (UTHealth) for GNP-KRAS samples. This work was supported by grants from the Cancer Prevention and Research Institute of Texas (CPRIT grant numbers DP150093 and RP190366). J.A.F. and Y.Z. are supported by the Department of Defense Breast Cancer Research Program (grant number W81XWH-20-1-0004). A.K.G. was supported by a postdoctoral training fellowship from the Keck Center Computational Cancer Biology Training Program (CCBTP) of the Gulf Coast Consortia (CPRIT grant no. RP170593).

■ REFERENCES

(1) Bos, J. L.; Rehmann, H.; Wittinghofer, A. Gefs and Gaps: Critical Elements in the Control of Small G Proteins. *Cell* **2007**, *129*, 865−877.

(2) Hobbs, G. A.; Der, C. J.; Rossman, K. L. Ras Isoforms and Mutations in Cancer at a Glance. *J. Cell Sci.* **2016**, *129*, 1287.

(3) Cox, A. D.; Der, C. J. Ras History: The Saga Continues. *Small GTPases* **2010**, *1*, 2−27.
(4) Herdeis, L.; Gerlach, D.; McConnell, D. B.; Kessler, D. Stopping the Beating Heart of Cancer: Kras Reviewed. *Curr. Opin. Struct. Biol.* **2021**, *71*, 136−147.
(5) Cox, A. D.; Fesik, S. W.; Kimmelman, A. C.; Luo, J.; Der, C. J. Drugging the Undruggable Ras: Mission Possible? *Nat. Rev. Drug. Discov.* **2014**, *13*, 828−851.
(6) John, J.; Sohmen, R.; Feuerstein, J.; Linke, R.; Wittinghofer, A.; Goody, R. S. Kinetics of Interaction of Nucleotides with Nucleotide-Free H-Ras P21. *Biochemistry* **1990**, *29*, 6058−6065.
(7) Feuerstein, J.; Goody, R. S.; Wittinghofer, A. Preparation and Characterization of Nucleotide-Free and Metal Ion-Free P21 "Apoprotein". *J. Biol. Chem.* **1987**, *262*, 8455−8458.
(8) Erickson, K. E.; Rukhlenko, O. S.; Posner, R. G.; Hlavacek, W. S.; Kholodenko, B. N. New Insights into Ras Biology Reinvigorate Interest in Mathematical Modeling of Ras Signaling. *Semin. Cancer Biol.* **2019**, *54*, 162−173.
(9) Traut, T. W. Physiological Concentrations of Purines and Pyrimidines. *Mol. Cell. Biochem.* **1994**, *140*, 1−22.
(10) Trahey, M.; McCormick, F. A Cytoplasmic Protein Stimulates Normal N-Ras P21 Gtpase, but Does Not Affect Oncogenic Mutants. *Science* **1987**, *238*, 542−545.
(11) Prakash, P.; Hancock, J. F.; Gorfe, A. A. Binding Hotspots on K-Ras: Consensus Ligand Binding Sites and Other Reactive Regions from Probe-Based Molecular Dynamics Analysis. *Proteins* **2015**, *83*, 898−909.
(12) Grant, B. J.; Lukman, S.; Hocker, H. J.; Sayyah, J.; Brown, J. H.; McCammon, J. A.; Gorfe, A. A. Novel Allosteric Sites on Ras for Lead Generation. *PLoS One* **2011**, *6*, No. e25711.
(13) Grant, B. J.; Gorfe, A. A.; McCammon, J. A. Ras Conformational Switching: Simulating Nucleotide-Dependent Conformational Transitions with Accelerated Molecular Dynamics. *PLoS Comput. Biol.* **2009**, *5*, No. e1000325.
(14) Gorfe, A. A.; Grant, B. J.; McCammon, J. A. Mapping the Nucleotide and Isoform-Dependent Structural and Dynamical Features of Ras Proteins. *Structure* **2008**, *16*, 885−896.
(15) Ganesan, A.; Coote, M. L.; Barakat, K. Molecular Dynamics-Driven Drug Discovery: Leaping Forward with Confidence. *Drug Discov. Today* **2017**, *22*, 249−269.
(16) Durrant, J. D.; McCammon, J. A. Molecular Dynamics Simulations and Drug Discovery. *BMC Biol.* **2011**, *9*, 71.
(17) Buhrman, G.; O'Connor, C.; Zerbe, B.; Kearney, B. M.; Napoleon, R.; Kovrigina, E. A.; Vajda, S.; Kozakov, D.; Kovrigin, E. L.; Mattos, C. Analysis of Binding Site Hot Spots on the Surface of Ras Gtpase. *J. Mol. Biol.* **2011**, *413*, 773−789.
(18) Kessler, D.; Bergner, A.; Böttcher, J.; Fischer, G.; Döbel, S.; Hinkel, M.; Müllauer, B.; Weiss-Puxbaum, A.; McConnell, D. B. Drugging All Ras Isoforms with One Pocket. *Future Med. Chem.* **2020**, *12*, 1911−1923.
(19) Gupta, A. K.; Wang, X.; Pagba, C. V.; Prakash, P.; Sarkar-Banerjee, S.; Putkey, J.; Gorfe, A. A. Multi-Target, Ensemble-Based Virtual Screening Yields Novel Allosteric Kras Inhibitors at High Success Rate. *Chem. Biol. Drug Des.* **2019**, *94*, 1441−1456.
(20) Kessler, D.; Gmachl, M.; Mantoulidis, A.; Martin, L. J.; Zoephel, A.; Mayer, M.; Gollner, A.; Covini, D.; Fischer, S.; Gerstberger, T.; Gmaschitz, T.; Goodwin, C.; Greb, P.; Häring, D.; Hela, W.; Hoffmann, J.; Karolyi-Oezguer, J.; Knesl, P.; Kornigg, S.; Koegl, M.; Kousek, R.; Lamarre, L.; Moser, F.; Munico-Martinez, S.; Peinsipp, C.; Phan, J.; Rinnenthal, J.; Sai, J.; Salamon, C.; Scherbantin, Y.; Schipany, K.; Schnitzer, R.; Schrenk, A.; Sharps, B.; Siszler, G.; Sun, Q.; Waterson, A.; Wolkerstorfer, B.; Zeeb, M.; Pearson, M.; Fesik, S. W.; McConnell, D. B. Drugging an Undruggable Pocket on Kras. *Proc. Natl. Acad. Sci. U.S.A.* **2019**, *116*, 15823.
(21) McCarthy, M. J.; Pagba, C. V.; Prakash, P.; Naji, A. K.; van der Hoeven, D.; Liang, H.; Gupta, A. K.; Zhou, Y.; Cho, K.-J.; Hancock, J. F.; Gorfe, A. A. Discovery of High-Affinity Noncovalent Allosteric Kras Inhibitors That Disrupt Effector Binding. *ACS Omega* **2019**, *4*, 2921−2930.
(22) Quevedo, C. E.; Cruz-Migoni, A.; Bery, N.; Miller, A.; Tanaka, T.; Petch, D.; Bataille, C. J. R.; Lee, L. Y. W.; Fallon, P. S.; Tulmin, H.; Ehebauer, M. T.; Fernandez-Fuentes, N.; Russell, A. J.; Carr, S. B.; Phillips, S. E. V.; Rabbitts, T. H. Small Molecule Inhibitors of Ras-Effector Protein Interactions Derived Using an Intracellular Antibody Fragment. *Nat. Commun.* **2018**, *9*, 3169.
(23) Spencer-Smith, R.; Koide, A.; Zhou, Y.; Eguchi, R. R.; Sha, F.; Gajwani, P.; Santana, D.; Gupta, A.; Jacobs, M.; Herrero-Garcia, E.; Cobbert, J.; Lavoie, H.; Smith, M.; Rajakulendran, T.; Dowdell, E.; Okur, M. N.; Dementieva, I.; Sicheri, F.; Therrien, M.; Hancock, J. F.; Ikura, M.; Koide, S.; O'Bryan, J. P. Inhibition of Ras Function through Targeting an Allosteric Regulatory Site. *Nat. Chem. Biol.* **2017**, *13*, 62−68.
(24) Hocker, H. J.; Cho, K. J.; Chen, C. Y.; Rambahal, N.; Sagineedu, S. R.; Shaari, K.; Stanslas, J.; Hancock, J. F.; Gorfe, A. A. Andrographolide Derivatives Inhibit Guanine Nucleotide Exchange and Abrogate Oncogenic Ras Function. *Proc. Natl. Acad. Sci. U.S.A.* **2013**, *110*, 10201−10206.
(25) Ostrem, J. M.; Peters, U.; Sos, M. L.; Wells, J. A.; Shokat, K. M. K-Ras(G12c) Inhibitors Allosterically Control Gtp Affinity and Effector Interactions. *Nature* **2013**, *503*, 548−551.
(26) Shima, F.; Yoshikawa, Y.; Ye, M.; Araki, M.; Matsumoto, S.; Liao, J.; Hu, L.; Sugimoto, T.; Ijiri, Y.; Takeda, A.; Nishiyama, Y.; Sato, C.; Muraoka, S.; Tamura, A.; Osoda, T.; Tsuda, K.-i.; Miyakawa, T.; Fukunishi, H.; Shimada, J.; Kumasaka, T.; Yamamoto, M.; Kataoka, T. In Silico Discovery of Small-Molecule Ras Inhibitors That Display Antitumor Activity by Blocking the Ras-Effector Interaction. *Proc. Natl. Acad. Sci. U.S.A.* **2013**, *110*, 8182−8187.
(27) Maurer, T.; Garrenton, L. S.; Oh, A.; Pitts, K.; Anderson, D. J.; Skelton, N. J.; Fauber, B. P.; Pan, B.; Malek, S.; Stokoe, D.; Ludlam, M. J. C.; Bowman, K. K.; Wu, J.; Giannetti, A. M.; Starovasnik, M. A.; Mellman, I.; Jackson, P. K.; Rudolph, J.; Wang, W.; Fang, G. Small-Molecule Ligands Bind to a Distinct Pocket in Ras and Inhibit Sos-Mediated Nucleotide Exchange Activity. *Proc. Natl. Acad. Sci. U.S.A.* **2012**, *109*, 5299−5304.
(28) Sun, Q.; Burke, J. P.; Phan, J.; Burns, M. C.; Olejniczak, E. T.; Waterson, A. G.; Lee, T.; Rossanese, O. W.; Fesik, S. W. Discovery of Small Molecules That Bind to K-Ras and Inhibit Sos-Mediated Activation. *Angew. Chem., Int. Ed. Engl.* **2012**, *51*, 6140−6143.
(29) Schmidtke, P.; Bidon-Chanal, A.; Luque, F. J.; Barril, X. Mdpocket: Open-Source Cavity Detection and Characterization on Molecular Dynamics Trajectories. *Bioinformatics* **2011**, *27*, 3276−3285.
(30) Molina-Arcas, M.; Samani, A.; Downward, J. Drugging the Undruggable: Advances on Ras Targeting in Cancer. *Genes* **2021**, *12*, 899.
(31) Fell, J. B.; Fischer, J. P.; Baer, B. R.; Blake, J. F.; Bouhana, K.; Briere, D. M.; Brown, K. D.; Burgess, L. E.; Burns, A. C.; Burkard, M. R.; Chiang, H.; Chicarelli, M. J.; Cook, A. W.; Gaudino, J. J.; Hallin, J.; Hanson, L.; Hartley, D. P.; Hicken, E. J.; Hingorani, G. P.; Hinklin, R. J.; Mejia, M. J.; Olson, P.; Otten, J. N.; Rhodes, S. P.; Rodriguez, M. E.; Savechenkov, P.; Smith, D. J.; Sudhakar, N.; Sullivan, F. X.; Tang, T. P.; Vigers, G. P.; Wollenberg, L.; Christensen, J. G.; Marx, M. A. Identification of the Clinical Development Candidate Mrtx849, a Covalent Krasg12c Inhibitor for the Treatment of Cancer. *J. Med. Chem.* **2020**, *63*, 6679−6693.
(32) Lanman, B. A.; Allen, J. R.; Allen, J. G.; Amegadzie, A. K.; Ashton, K. S.; Booker, S. K.; Chen, J. J.; Chen, N.; Frohn, M. J.; Goodman, G.; Kopecky, D. J.; Liu, L.; Lopez, P.; Low, J. D.; Ma, V.; Minatti, A. E.; Nguyen, T. T.; Nishimura, N.; Pickrell, A. J.; Reed, A. B.; Shin, Y.; Siegmund, A. C.; Tamayo, N. A.; Tegley, C. M.; Walton, M. C.; Wang, H. L.; Wurz, R. P.; Xue, M.; Yang, K. C.; Achanta, P.; Bartberger, M. D.; Canon, J.; Hollis, L. S.; McCarter, J. D.; Mohr, C.; Rex, K.; Saiki, A. Y.; San Miguel, T.; Volak, L. P.; Wang, K. H.; Whittington, D. A.; Zech, S. G.; Lipford, J. R.; Cee, V. J. Discovery of a Covalent Inhibitor of KRASG12C (AMG 510) for the Treatment of Solid Tumors. *J. Med. Chem.* **2020**, *63*, 52−65.
(33) Stephen, A. G.; Esposito, D.; Bagni, R. K.; McCormick, F. Dragging Ras Back in the Ring. *Cancer Cell* **2014**, *25*, 272−281.

https://doi.org/10.1021/acsbiomedchemau.2c00045
ACS Bio Med Chem Au 2022, 2, 617−626

(34) Bery, N.; Cruz-Migoni, A.; Bataille, C. J.; Quevedo, C. E.; Tulmin, H.; Miller, A.; Russell, A.; Phillips, S. E.; Carr, S. B.; Rabbitts, T. H. Bret-Based Ras Biosensors That Show a Novel Small Molecule Is an Inhibitor of Ras-Effector Protein-Protein Interactions. *Elife* **2018**, *7*, No. e37122.
(35) Cruz-Migoni, A.; Canning, P.; Quevedo, C. E.; Bataille, C. J. R.; Bery, N.; Miller, A.; Russell, A. J.; Phillips, S. E. V.; Carr, S. B.; Rabbitts, T. H. Structure-Based Development of New Ras-Effector Inhibitors from a Combination of Active and Inactive Ras-Binding Compounds. *Proc. Natl. Acad. Sci. U.S.A.* **2019**, *116*, 2545−2550.
(36) Welsch, M. E.; Kaplan, A.; Chambers, J. M.; Stokes, M. E.; Bos, P. H.; Zask, A.; Zhang, Y.; Sanchez-Martin, M.; Badgley, M. A.; Huang, C. S.; Tran, T. H.; Akkiraju, H.; Brown, L. M.; Nandakumar, R.; Cremers, S.; Yang, W. S.; Tong, L.; Olive, K. P.; Ferrando, A.; Stockwell, B. R. Multivalent Small-Molecule Pan-Ras Inhibitors. *Cell* **2017**, *168*, 878−889.
(37) Huynh, K.; Partch, C. L. Analysis of Protein Stability and Ligand Interactions by Thermal Shift Assay. *Curr. Protoc. Protein Sci.* **2015**, *79*, 28.9.1−28.9.14.
(38) Lo, M. C.; Aulabaugh, A.; Jin, G.; Cowling, R.; Bard, J.; Malamas, M.; Ellestad, G. Evaluation of Fluorescence-Based Thermal Shift Assays for Hit Identification in Drug Discovery. *Anal. Biochem.* **2004**, *332*, 153−159.
(39) Kauke, M. J.; Traxlmayr, M. W.; Parker, J. A.; Kiefer, J. D.; Knihtila, R.; McGee, J.; Verdine, G.; Mattos, C.; Wittrup, K. D. An Engineered Protein Antagonist of K-Ras/B-Raf Interaction. *Sci. Rep.* **2017**, *7*, 5831.
(40) Xu, S.; Long, B. N.; Boris, G. H.; Chen, A.; Ni, S.; Kennedy, M. A. Structural Insight into the Rearrangement of the Switch I Region in Gtp-Bound G12a K-Ras. *Acta Crystallogr., Sect. D: Struct. Biol.* **2017**, *73*, 970−984.
(41) Hunter, J. C.; Manandhar, A.; Carrasco, M. A.; Gurbani, D.; Gondi, S.; Westover, K. D. Biochemical and Structural Analysis of Common Cancer-Associated Kras Mutations. *Mol. Cancer Res.* **2015**, *13*, 1325−1335.
(42) Marcus, K.; Mattos, C. Direct Attack on Ras: Intramolecular Communication and Mutation-Specific Effects. *Clin. Cancer Res.* **2015**, *21*, 1810.
(43) Ford, B.; Skowronek, K.; Boykevisch, S.; Bar-Sagi, D.; Nassar, N. Structure of the G60a Mutant of Ras: Implications for the Dominant Negative Effect. *J. Biol. Chem.* **2005**, *280*, 25697−25705.
(44) Lu, S.; Jang, H.; Muratcioglu, S.; Gursoy, A.; Keskin, O.; Nussinov, R.; Zhang, J. Ras Conformational Ensembles, Allostery, and Signaling. *Chem. Rev.* **2016**, *116*, 6607−6665.
(45) Vetter, I. R.; Wittinghofer, A. Signal Transduction - the Guanine Nucleotide-Binding Switch in Three Dimensions. *Science* **2001**, *294*, 1299−1304.
(46) Milburn, M. V.; Tong, L.; deVos, A. M.; Brünger, A.; Yamaizumi, Z.; Nishimura, S.; Kim, S. H. Molecular Switch for Signal Transduction: Structural Differences between Active and Inactive Forms of Protooncogenic Ras Proteins. *Science* **1990**, *247*, 939.
(47) Boriack-Sjodin, P. A.; Margarit, S. M.; Bar-Sagi, D.; Kuriyan, J. The Structural Basis of the Activation of Ras by Sos. *Nature* **1998**, *394*, 337−343.
(48) Lenzen, C.; Cool, R. H.; Prinz, H.; Kuhlmann, J.; Wittinghofer, A. Kinetic Analysis by Fluorescence of the Interaction between Ras and the Catalytic Domain of the Guanine Nucleotide Exchange Factor Cdc25mm. *Biochemistry* **1998**, *37*, 7420−7430.
(49) Patgiri, A.; Yadav, K. K.; Arora, P. S.; Bar-Sagi, D. An Orthosteric Inhibitor of the Ras-Sos Interaction. *Nat. Chem. Biol.* **2011**, *7*, 585.
(50) Fetics, S. K.; Guterres, H.; Kearney, B. M.; Buhrman, G.; Ma, B.; Nussinov, R.; Mattos, C. Allosteric Effects of the Oncogenic Rasq61l Mutant on Raf-Rbd. *Structure* **2015**, *23*, 505−516.
(51) Kattan, W. E.; Liu, J.; Montufar-Solis, D.; Liang, H.; Brahmendra Barathi, B.; van der Hoeven, R.; Zhou, Y.; Hancock, J. F. Components of the Phosphatidylserine Endoplasmic Reticulum to Plasma Membrane Transport Mechanism as Targets for Kras Inhibition in Pancreatic Cancer. *Proc. Natl. Acad. Sci. U.S.A.* **2021**, *118*, No. e2114126118.
(52) Ahmed, D.; Eide, P. W.; Eilertsen, I. A.; Danielsen, S. A.; Eknæs, M.; Hektoen, M.; Lind, G. E.; Lothe, R. A. Epigenetic and Genetic Features of 24 Colon Cancer Cell Lines. *Oncogenesis* **2013**, *2*, No. e71.
(53) Berrozpe, G.; Schaeffer, J.; Peinado, M. A.; Real, F. X.; Perucho, M. Comparative Analysis of Mutations in the P53 and K-Ras Genes in Pancreatic Cancer. *Int. J. Cancer* **1994**, *58*, 185−191.
(54) Yunis, A. A.; Arimura, G. K.; Russin, D. J. Human Pancreatic Carcinoma (Mia Paca-2) in Continuous Culture: Sensitivity to Asparaginase. *Int. J. Cancer* **1977**, *19*, 128−135.
(55) Pollard, T. D. A Guide to Simple and Informative Binding Assays. *Mol. Biol. Cell* **2010**, *21*, 4061−4067.
(56) Marchand, J.-B.; Kaiser, D. A.; Pollard, T. D.; Higgs, H. N. Interaction of Wasp/Scar Proteins with Actin and Vertebrate Arp2/3 Complex. *Nat. Cell Biol.* **2001**, *3*, 76−82.

https://doi.org/10.1021/acsbiomedchemau.2c00045
ACS Bio Med Chem Au 2022, 2, 617−626